A closer look into metastable effects of $Cu(In,Ga)Se_2$ solar cells

Condensed Matter Journal Club

Collin Brown

Dec 7th, 2017

T. Lavrenko, T. Walter and B. Plesz, "A closer look into metastable effects of $Cu(In,Ga)Se_2$ solar cells," *Phys. Status Solidi C*, **14**(6), 1600197 (2017).

Cu(In,Ga)Se2 Solar Cells

- 2nd Generation – Thin Film solar cells
- Metastability
  - Selenium-Copper vacancy complex – Lany-Zunger
  - Movement of ions within the lattice – Sodium and others
  - “Due to its amphoteric nature, the (VSe-VCu) complex is able to convert by persistent carrier capture or emission from a shallow donor into a shallow acceptor configuration, and vice versa, thereby changing in a metastable fashion the local net acceptor density inside the CIGS absorber of the solar cell, e.g., a CdS/CIGS heterojunction. “[1]

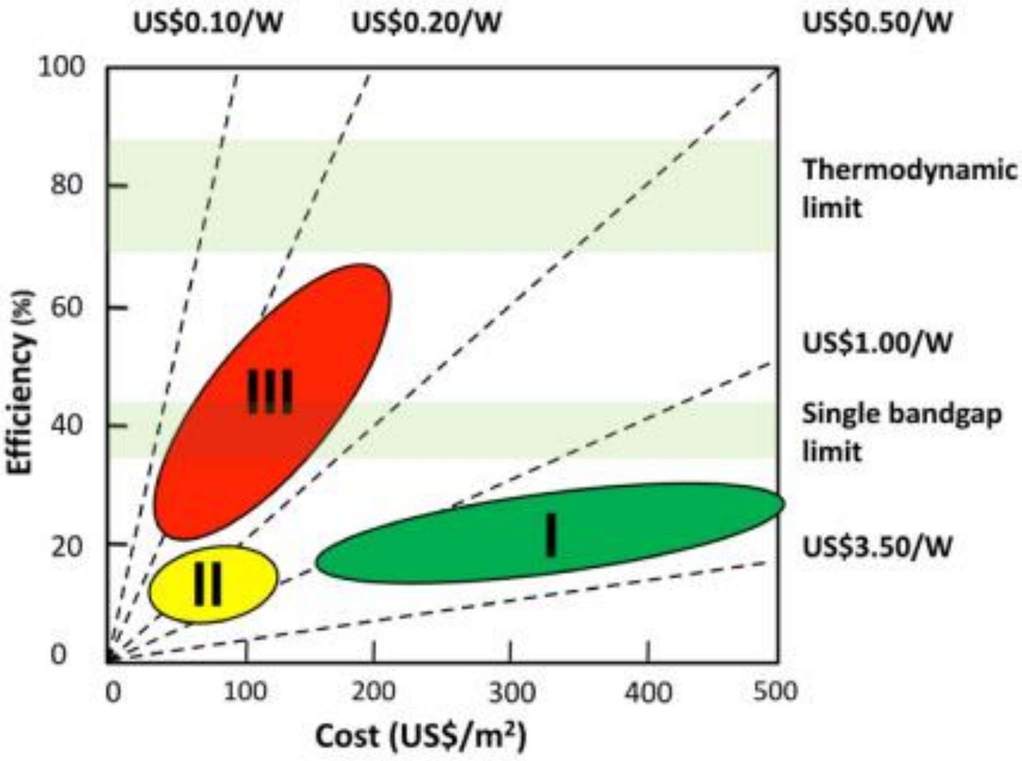

---

[1] S. Lany and A. Zunger, "Light- and bias-induced metastabilities in Cu(In,Ga)Se2 based solar cells caused by the (VSe-VCu) vacancy complex," *Journal of Applied Physics*, vol. 100, p. 113725, 2006/12/01 2006.

[2] Green, M. A. (2001), Third generation photovoltaics: Ultra-high conversion efficiency at low cost. Prog. Photovolt: Res. Appl., 9: 123–135. doi:10.1002/pip.360

Photoluminescence Imaging

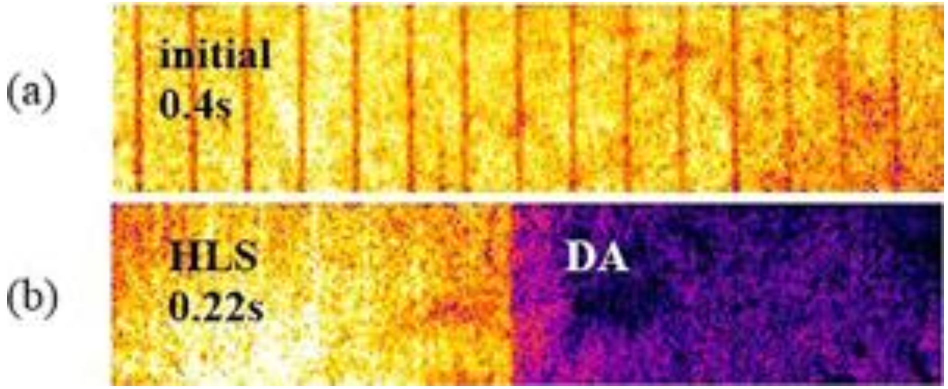

Figure 2 - Steady-state PL images of the CIGS/CdS sample in the initial state (a) and after local HLS for 3.5 h at 100 °C (b).

- PL intensity $\propto$ Spontaneous Emission Rate
- Imaging can give insight to splitting of quasi-Fermi levels, minority carrier lifetimes, and others
- Here, the samples were excited by LED arrays with 625 nm and 465 nm LEDs.
- PL intensity can be affected by carrier lifetimes and internal electric fields

Vibrating Kelvin Probe

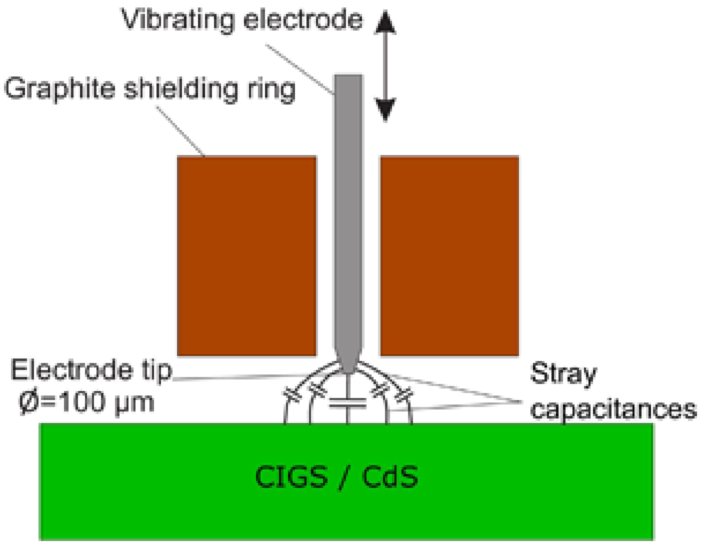

Figure 1 – Schematic representation of the vibrating Kelvin probe arrangement used in this work.

- 2 connected materials with different work functions produce a built in electric potential.
- The electrode introduces an electric field, which induces AC current due to the electrode vibrating. When the electric field compensates the built in potential, the induced AC current is 0, and the field is the same as the work function difference.
- Surface Potential variations can be detected.

Hot Light Soaking

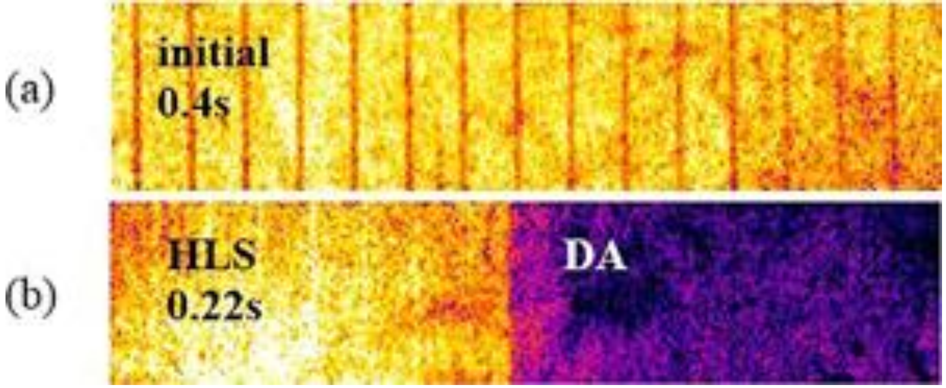

Figure 2 - Steady-state PL images of the CIGS/CdS sample in the initial state (a) and after local HLS for 3.5 h at 100 °C (b).

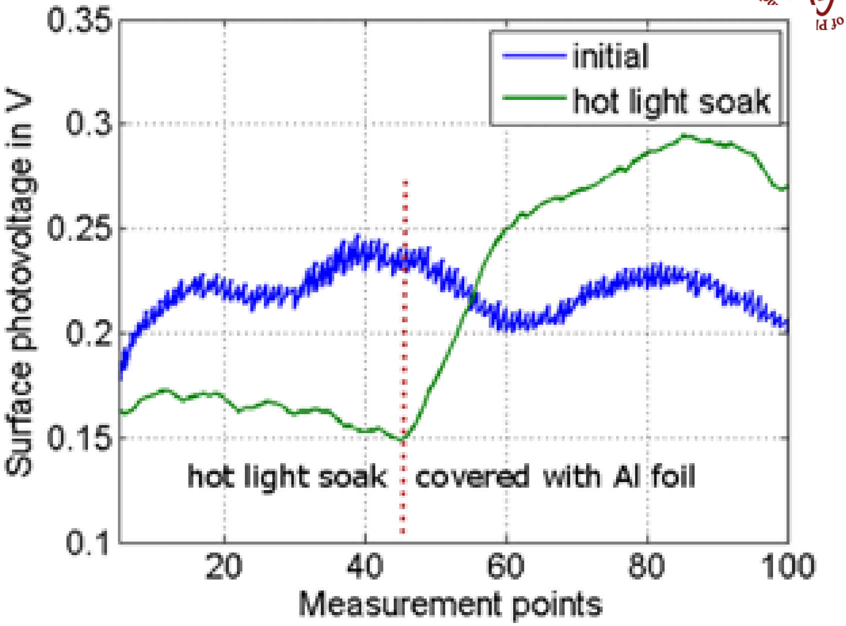

Figure 3 - Line scan of the surface photovoltage under white light illumination in the initial state and after HLS.

Both sides of same endure heat treatment, while only 1 side is light soaked.

- Heat treatment appears to enhance surface band bending. Increase of Surface Photovoltage and quenching of PL.

- Hot Light Soak leads to a partial band flattening. Decrease of Surface Photovoltage and increase in PL

Thermal Treatment

- The sample was kept in an elevated temp environment, and degradation was enforced on only one side of the sample.
- Areas with Higher PL intensity show up as areas with lower potential in (b).

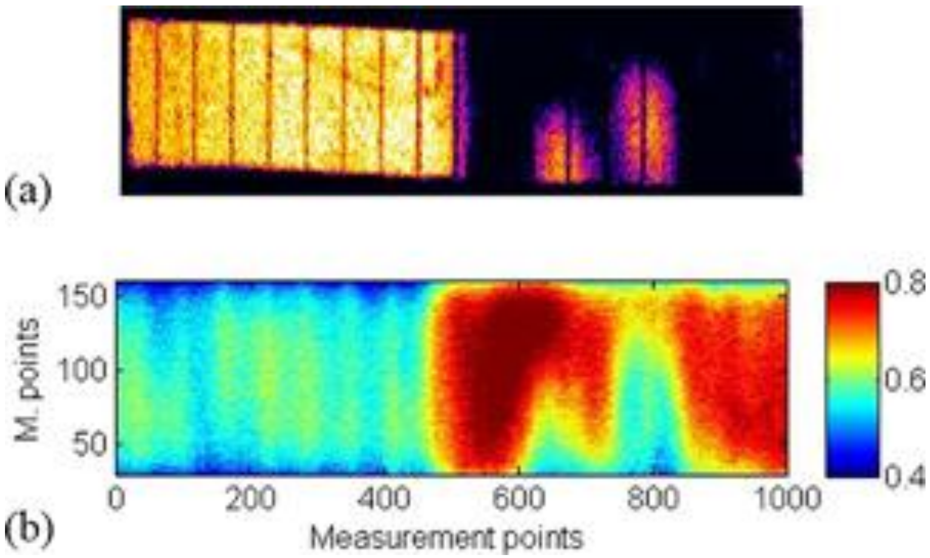

Figure 4 - Steady-state PL image (a) and mapping of surface potential variations (b) of the CIGS/CdS sample (stepsize of 64 microns) after local degradation.

Etching of CdS Buffer layer

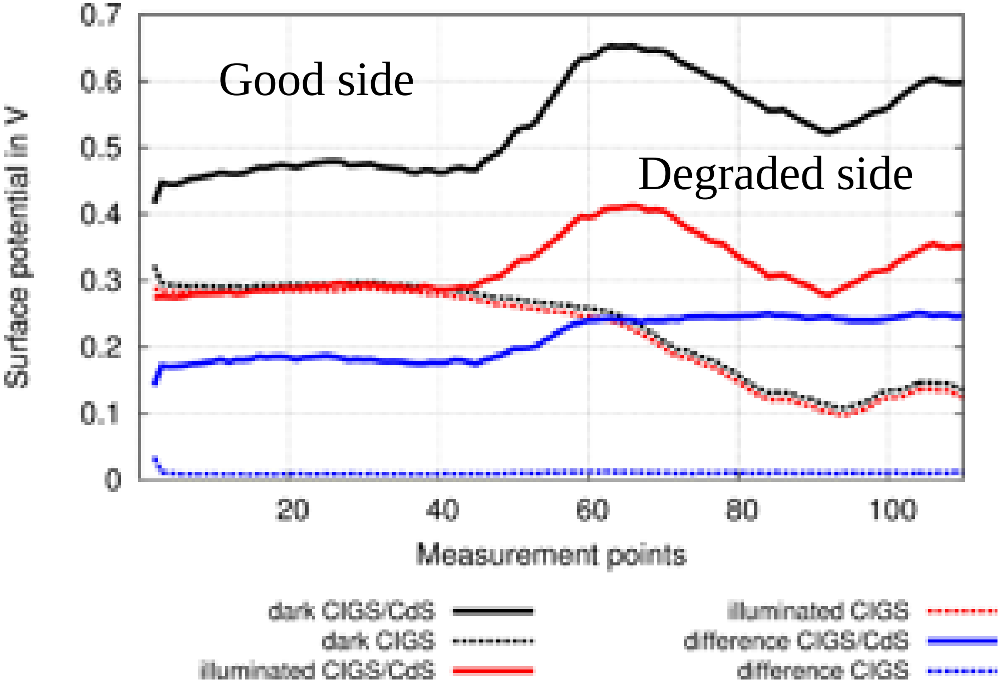

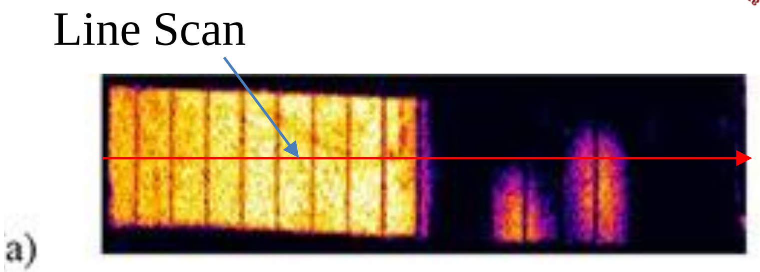

Figure 5 - Line scan of the surface potential in the dark (black), under white light illumination (red) and the difference between the two (blue). Solid lines correspond to the measurements on the CIGS/CdS heterostructure, whereas dotted lines correspond to the measurements on the bare CIGS absorber.

- Sample was Etched after the Thermal treatment by a 5% solution of HCl for 3 min.
- Removing the Buffer layer eliminates the photovoltage difference, possibly indicating charge buildup at the buffer absorber interface causing the observed metastability.
- Removing the Buffer layer also cause a large change in the absolute photovoltage on the degraded side, which will be studied separately.

Etching of CdS Buffer layer

- Directly after light soaking, the sample is etched in 5% HCl for 5 min to removed the buffer layer, and then imaged.
- The difference between the PL intensities on the 2 sides has been removed, similar to what was seen in the line scan.
- CdS layer and/or interface contributes significantly to observed metastability

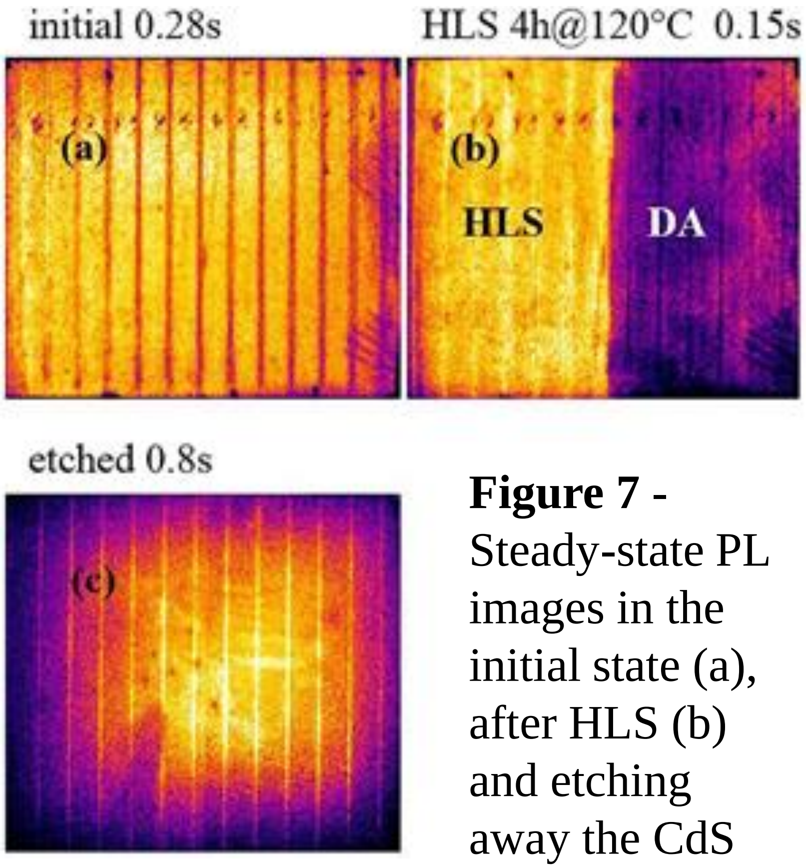

Figure 7 - Steady-state PL images in the initial state (a), after HLS (b) and etching away the CdS buffer layer (c).

P1 Scribe

- "In a typical CIGS process, a laser is used to segment the first conductive layer (P1), typically Molybdenum (Mo), into adjacent, electrically isolated strips (or bands)."[3]
- Stronger band bending in the vicinity of the scribes, but under illumination the difference disappears.

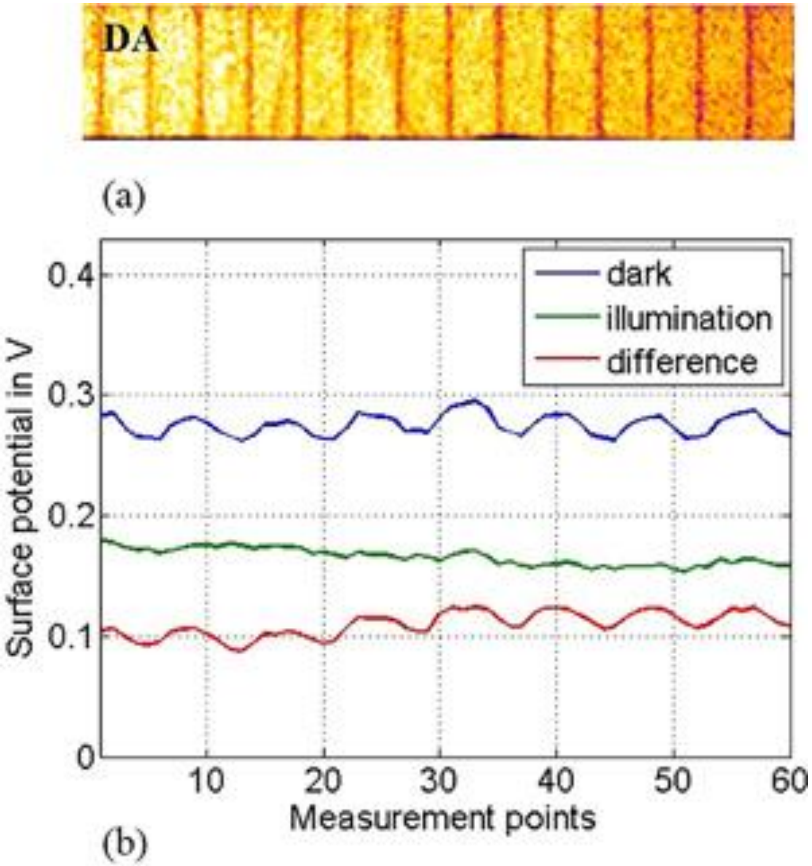

Figure 6 - Steady-state PL image (a) and line scan of the surface potentials (b) in the dark (blue), under white light illumination (green) and the difference between them (red) after dark annealing CIGS/CdS sample at 130 °C for 24 h.

[3] Rekow M, Murison R, Dunsky C, Dinkel C, Pern J, Mansfield L, Panarello T, Nikumb S. CIGS P1, P2, P3 scribing processes using a pulse programmable industrial fiber laser. Proceedings of 25th European Photovoltaic Solar Energy Conference and Exhibition, Valencia, Spain: 6-10 Sept. 2010; p. 2862–2871.

Conclusions

treatm./param.	hot light soak	heat treatment	HCl-etching
band bending	flattening	enhancement	flattening
PL intensity	enhancement	quenching	difference vanishes

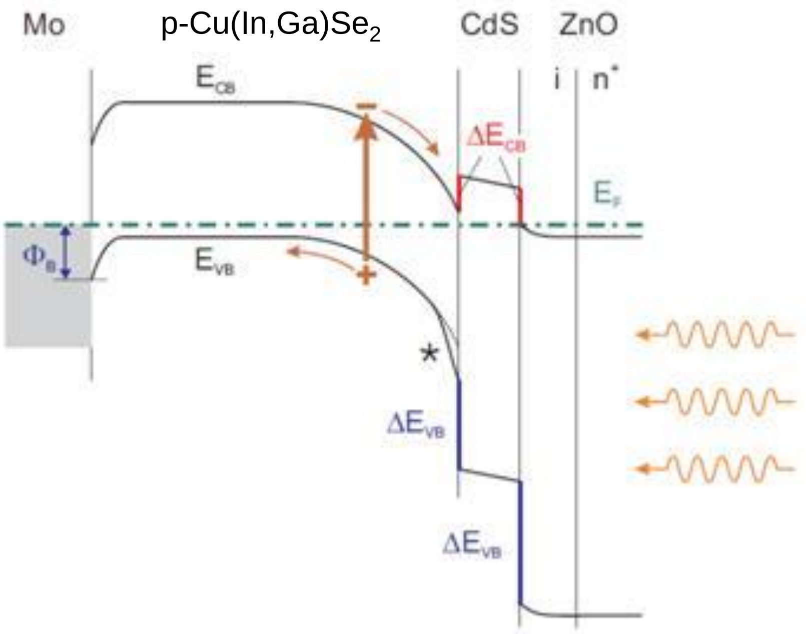

- CdS layer and interface can have a large effect on observed metastability in these devices.
- P1 patterning must be designed properly to not adversely affect the cell performance.